Emergent Materials (2019) 2:209–217
https://doi.org/10.1007/s42247-019-00037-5

ORIGINAL ARTICLE

Strategies to prevent dopamine oxidation and related cytotoxicity using various antioxidants and nitrogenation

Devyesh Rana[1] · Thibault Colombani[1] · Halimatu S. Mohammed[1] · Loek J. Eggermont[1] · Samantha Johnson[2] · Nasim Annabi[1,3,4,5] · Sidi A. Bencherif[1,2,6,7]

Received: 30 May 2019 / Accepted: 28 June 2019 / Published online: 7 August 2019

Abstract

Dopamine (DA) plays several important roles in the brain and body and has recently been used as a bioadhesive precursor for medical applications. However, DA oxidizes immediately when exposed to oxygen and rapidly polymerizes into polydopamine (PDA), leading to oxidative stress, cytotoxicity, and loss of DA functionalities. As a result, preventing rapid oxidation of DA is of paramount importance but still remains a major challenge. Here, we report several strategies to impede DA oxidation in relevant aqueous solutions (i.e., water, PBS, and cell culture media). One strategy is based on using reducing agents or antioxidants such as glutathione in its reduced state (GSH) and sodium tetraborate (commonly known as borax). Another strategy is based on nitrogenation, a method used to preserve DA in its reduced form by creating an oxygen-free environment. Our data suggest that the antioxidant properties of GSH and borax substantially decreased DA oxidation for up to 2 months. Nitrogenation or oxygen removal further prevented DA oxidation, enhancing its shelf life for longer periods of time. When tested with mammalian cells, preventing DA oxidation with GSH dramatically improved viability of 3T3 fibroblasts and T cells. These results demonstrate that the use of antioxidants, alone or in combination with nitrogenation, can help prevent DA oxidation and improve its stability for cell-based studies or for the design and development of biomaterials.

Keywords Dopamine · Oxidation · Reducing agents · Nitrogenation · Cytocompatibility

1 Introduction

Dopamine (DA), an innate catecholaminergic neurotransmitter, and its oxidized derivatives, including polydopamine (PDA), are of interest for their role in several biological processes and diseases [1–5]. For instance, DA oxidation, low DA concentrations, and high PDA concentrations are indicators of neurological conditions, including Parkinson's and Alzheimer's diseases [6]. Biological processes regulate DA oxidation and its conversion into PDA to combat the onset of these diseases [7]. In addition to these functionalities, evidence from clinical studies in humans suggests that a subunit

Electronic supplementary material The online version of this article (https://doi.org/10.1007/s42247-019-00037-5) contains supplementary material, which is available to authorized users.

✉ Nasim Annabi
nannabi@ucla.edu

✉ Sidi A. Bencherif
s.bencherif@northeastern.edu

[1] Department of Chemical Engineering, Northeastern University, Boston, MA, USA

[2] Department of Bioengineering, Northeastern University, Boston, MA, USA

[3] Harvard-MIT Division of Health Sciences and Technology, Massachusetts Institute of Technology, Cambridge, MA, USA

[4] Department of Chemical and Biomolecular Engineering, University of California, Los Angeles, Los Angeles, CA 90095, USA

[5] Center for Minimally Invasive Therapeutics (C-MIT), California NanoSystems Institute (CNSI), University of California, Los Angeles, Los Angeles, CA 90095, USA

[6] Harvard John A. Paulson School of Engineering and Applied Sciences, Harvard University, Cambridge, USA

[7] Sorbonne University, UTC CNRS UMR 7338, Biomechanics and Bioengineering (BMBI), University of Technology of Compiègne, Compiègne, France

of melanin polymerizes into PDA, which causes dark pigmentation on the skin, hair, and the substantia nigra of the brain [8]. However, in other organisms such as mussels, PDA plays a pivotal role in their adhesion in wet environments.

There are numerous reports on the rapid oxidation of DA under physiological pH [5, 7, 9] and its effect on several processes, including adhesiveness of biomaterials [5, 7, 10–12], therapeutics [1–3], and conductive and adhesive material coatings [4, 9, 13–15]. In the body, self-polymerization of DA into PDA occurs in the presence of oxygen or monoamine oxidase [10]. Furthermore, conversion of DA into PDA can be catalyzed by an oxidizing agent such as sodium periodate. This characteristic oxidation is qualitatively observed by the blackening of DA due to PDA formation, which has been associated with mammalian cell death [6, 8, 16–20]. There is a large body of evidence suggesting that PDA formation leads to oxidative stress–induced cytotoxicity due to the formation of free radicals [21]. Specifically, it was found that DA oxidation triggers apoptosis, while the use of antioxidants could prevent DA-related cytotoxicity [22]. Furthermore, PDA formation inhibits binding of DA to thiols, amines, and hydroxyls [10, 23]. Thus, there is an urgent need to develop or reinforce strategies to control the rapid oxidation of DA.

To address this oxidative challenge, Han et al. recently proposed a two-step polymerization technique to limit oxidation of dopamine by encapsulating DA in clay interlayers followed by controlled oxidation to form PDA [12]. However, steric hindrance and physical restrictions limited the ability of DA to directly interact with tissues in this strategy [12]. Here, we have investigated three facile routes to prevent DA oxidation in relevant aqueous solutions (water, phosphate buffered saline (PBS), and cell culture media). Specifically, we hypothesize that both glutathione (GSH), an antioxidant present in most mammalian tissues, and sodium tetraborate (borax), a chemically inert antioxidant, can be used independently and in combination with nitrogenation to preserve DA in its reduced state for further chemical modifications or to limit oxidative stress–induced cell toxicity.

2 Results and discussion

2.1 Rate of DA oxidation and PDA formation

To determine the rate of DA oxidation and PDA formation (Fig. 1), absorbance of unmodified DA in water, PBS (pH 7.4), and complete media were measured at various time points. UV-vis data was utilized and the rate of DA oxidation (r_{DA}) was derived from a plot showing the percentage of oxidized DA as a function of time. Within 1 h, low levels of DA oxidation were observed. The percentage of oxidation in water, PBS, and cell culture media was quantified to be 18.6% ± 9.6%, 13.3% ± 1.7%, and 16.6% ± 1.9%, respectively (Fig. 2). Prolonged incubation of DA-containing samples in their respective solvents intensified oxidation. Specifically, the percentage of oxidized DA significantly increased to 71.6% ± 8.6%, 74.3% ± 19.3%, and 92.7% ± 1.0% in water, PBS, and media, respectively, after 12 h.

Subsequently, the average reaction rate for DA oxidation at 37 °C was determined as shown in Eq. 1:

$$[\mathrm{DA}] = [\mathrm{DA}]_0 \times e^{k_{\mathrm{DA}}t}; k_{DA} = 3.28 \times 10^{-3}\mathrm{min}^{-1} \quad (1)$$

The oxidation of unmodified DA was visibly confirmed in all tested solutions (Fig. 2). DA in water and PBS resulted in 76.9% ± 19.3% and 76.9% ± 8.7% oxidation within 24 h. Interestingly, the highest oxidation rate was observed in cell culture media, in which DA was almost completely oxidized within the same time frame. These data can be fitted (correlation factor > 0.98) to Eq. 1. Furthermore, it was observed that DA consumption follows first-order kinetics as shown in Eq. 2:

$$[A] = [A]_0 \exp(-k_a t) \quad (2)$$

In this equation, $[A]$ is the final concentration of DA, $[A]_0$ is the starting concentration of DA, t is time, and k_a is the rate constant. The calculated $k_{\mathrm{DA}} = 3.28 \times 10^{-3} \pm 0.001.2 \times 10^{-3}$ min^{-1}, where the rate constant is the average of the three samples used and the error is the maximum deviation calculated with $n = 3$. The rate of oxidation is in line with the approximate simulated oxidation rate ($r_{\mathrm{DA}} = 4 \times 10^{-3}[\mathrm{DA}]^{1/2}$) [24]. To confirm this set of data, additional characterizations by ^{1}H nuclear magnetic resonance (NMR) spectroscopy Raman spectroscopy Fourier-transform infrared (FTIR), Spectroscopy and high-performance liquid chromatography (HPLC) are presented in the Supplementary Information (Figure S1 and Figure S2) [25]. In summary, these results confirmed the instability and rapid oxidation of unmodified DA and its conversion into PDA in various oxygen-containing and antioxidant-free aqueous solutions.

2.2 Effect of antioxidants on DA oxidation

Three different strategies were proposed to prevent and limit the rapid oxidation of DA. Specifically, nitrogenation was employed, as well as reduction reactions using two commonly used antioxidants, borax and GSH. These results were compared with ascorbic acid (AA), a gold standard antioxidant used here as a control. AA, also known as vitamin C, was used as it is and the most widely used antioxidant in cell-based in vitro studies. GSH was chosen for its high cytocompatibility and strong ability to reduce oxidative stress [26]. Although GSH has been used in a number of bioassays, there is limited data on its application for the stabilization of DA. Finally, borax is known to be toxic to cells, which limits its application for in vitro and in vivo studies. However, it

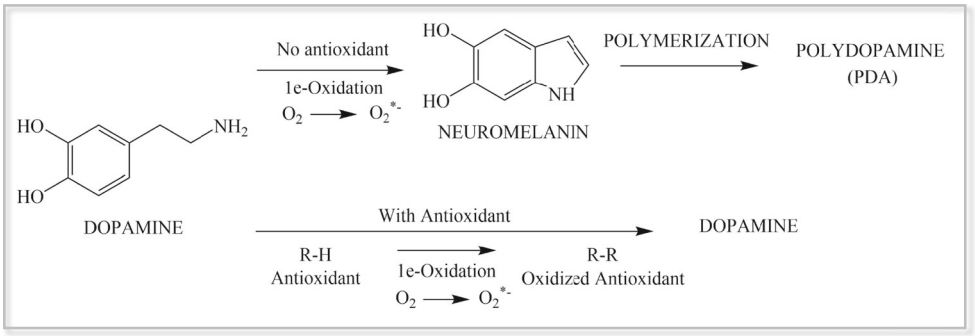

Fig. 1 Mechanisms of DA oxidation and strategies to prevent its alteration. Reaction mechanism for DA oxidation and subsequent polymerization generating PDA, as well as a strategy to retain DA in its reduced state using a potent antioxidant

could be used to stabilize DA in chemical synthesis–related applications. During the chemical modification of DA, borax has been used as an alternative to GSH to prevent unwanted competition between GSH and DA, as both contain similar reactive groups.

To this end, the onset of DA oxidation was studied over a 2-month period (56 days) and the results from both UV-vis measurements and visual analysis are shown in Fig. 3 a (i) and a (ii–iv), respectively. Briefly, 1 mM DA (1D, control), 1 mM DA supplemented with 20 mM GSH (D20G), and 1 mM DA supplemented with 20 mM borax (D20B) in PBS were investigated for long-term stability at 37 °C. These samples were investigated with and without nitrogenation to determine its efficacy in preventing DA oxidation. Samples were tested at 1, 3, 7, 14, 28, and 56 days. These time points in a geometric sequence were chosen to monitor DA oxidation over 2 months in an exponential growth model. The concentrations of borax used in these studies were chosen based on its solubility [27]. The use of higher concentrations resulted in limited solubility and precipitation of the antioxidant. Our results revealed a rapid oxidation of DA, reaching up to 90% oxidation within 2 days (Fig. 3a(i)). Specifically, the UV-vis

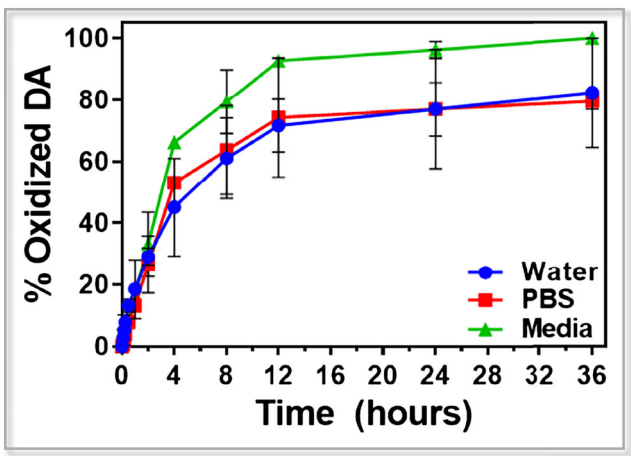

Fig. 2 DA readily oxidizes in different aqueous solutions: water, PBS, and cell culture media. UV absorbance of DA, expressed as % oxidized DA over time, is monitored at 530 nm using UV-vis spectroscopy. Values represent mean and SD ($n \geq 3$)

measurements showed a total oxidation for 1D of 95.9% ± 4.1% and this was visually confirmed as presented in Fig. 3a(ii). Conversely, after 24 h, DA oxidation was significantly reduced for D20B and D20G down to 3.2% ± 0.9% and nearly 0%, respectively. However, extended incubation for up to 56 days resulted in an increased oxidation of DA up to 21%. In solution, both GSH and borax can dissociate hydrogen ions to react with oxygen. This reaction is likely more favored than the oxidation of DA, which follows a more complex route and requires a higher activation energy [28].

These data suggest that both GSH and borax may be used to retain DA in its reduced state. Furthermore, antioxidant-free DA was found to darken quickly, which was consistent with previously reported findings for DA oxidation and PDA formation. However, based on our UV-vis data, even a slight oxidation of DA resulted in darkening [9, 20, 23, 29].

The last technique employed was nitrogenation, an approach to exchange oxygen with nitrogen to prevent oxidation. Although this method may not be suitable for cell-based studies, simple chemical synthesis as well as long-term storage of DA in different aqueous solutions may benefit from this technique. Specifically, samples were purged with nitrogen for approximately 30 min before and immediately after addition of DA with or without antioxidants and subsequently monitored for up to 2 months. In comparison with non-nitrogenated DA samples, all nitrogenated samples showed improved inhibition of DA oxidation (< 2%) (Fig. 3b(i)). These results were further confirmed visually, which is represented in Fig. 3b(ii–iv). The slight oxidation of DA that was observed is likely due to oxygen contamination during sample measurement and handling. This demonstrated that nitrogenation may be sufficient for retaining DA for an extended period of time. As a control, these results were compared with a solution of 1 mM DA supplemented with 1 mM AA (D1A), which has been reported as the maximum amount of AA tolerated by mammalian cells [30]. In cell culture media, D1A resulted in visible oxidation (33.1% ± 6.7%) as early as 24 h post-incubation. Complete DA oxidation was observed after 6 days (Figure S3). Remarkably, higher AA concentrations, equivalent to D20G and D20B, still resulted in high DA oxidation. Specifically, 1 mM DA supplemented with 20 mM AA

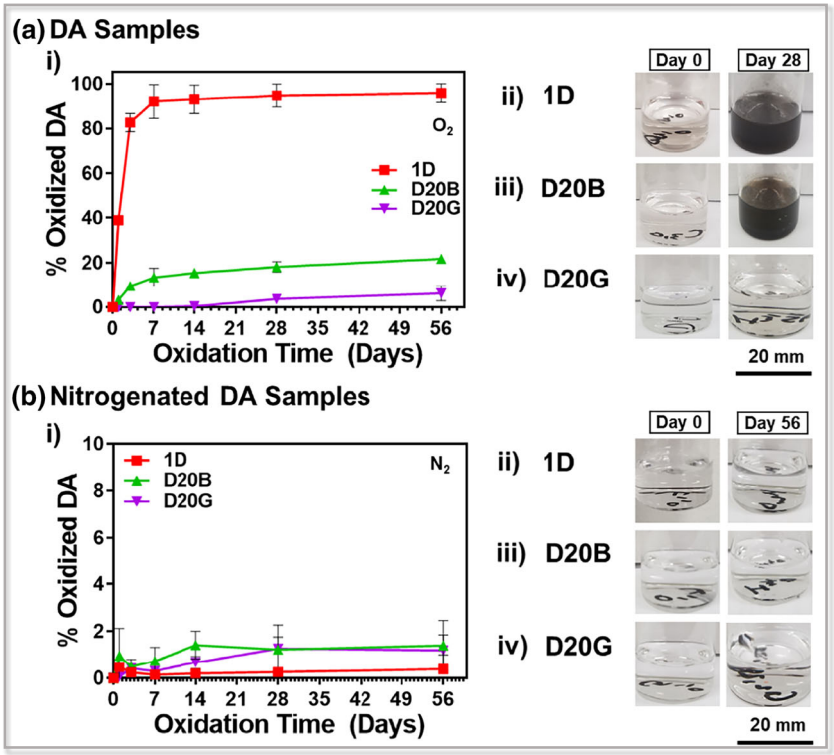

Fig. 3 Prevention of DA oxidation with antioxidants and nitrogenation. **a** Plot of DA oxidation in % with respect to time. (i) Quantitative data obtained from UV absorbance at 530 nm to record DA oxidation over time in normoxia. Representative images of (ii) 1D: 1 mM DA in PBS, (iii) D20B: 1 mM DA in 20 mM borax, and (iv) D20G: 1 mM DA in 20 mM GSH on days 0 and 28. **b** Quantitative data obtained from UV-vis absorbance at 530 nm to record DA oxidation over time in an oxygen-free environment (nitrogen purging). Representative images of (ii) 1D: 1 mM DA in nitrogen-purged PBS, (iii) D20B: 1 mM DA in nitrogen-purged 20 mM borax, and (iv) D20G: 1 mM DA in nitrogen-purged 20 mM GSH on days 0 and 56. Values represent mean and SD ($n \geq 3$)

(D20A) resulted in 86.7% ± 6.1% DA oxidation after 6 days, while only 5% of DA was oxidized for 20GSH (Figure S3). Furthermore, 10 mM GSH (10GSH) was also able to limit DA oxidation to levels below 10%.

This was confirmed by an observed slower reaction rate and rate constant (Eq. 3) of the DA oxidation reaction. Overall, the DA oxidation rate used is as follows:

$$[\mathrm{DA}] = -1.51 \times 10^{-5}[\mathrm{DA}]_0; k_{\mathrm{DA,Overall}} \text{ of } 1.51 \times 10^{-5}\mathrm{min}^{-1} \quad (3)$$

Data was fit to a linear regression and by averaging the slope from multiple experiments ($n = 3$) to ascertain $k_{\mathrm{DA,Overall}}$. This result was also confirmed by enzyme-linked immunosorbent assay (ELISA) (Figure S4). GSH concentrations above 20 mM resulted in its precipitation and aggregation and were not further considered for this reason. It should be noted that, for typical cell culture–related experiments, media is replaced within 5–7 days. This suggests that GSH may be a suitable antioxidant for cell-based in vitro studies due to its longer stability.

A schematic of the experimental setup to prevent DA oxidation with GSH and nitrogenation can be found in Figs. 4 and Figure S5, respectively. In particular, DA-containing samples that were treated using nitrogenation could be stored for over 2 months. For short-term storage or the chemical modification of DA, borax was a viable option for samples that are sensitive to functionalities of GSH (e.g., thiol, amine, or carboxylic acid groups). Specifically, for applications in Ni/Co supercapacitors or Fe-based anodes in which DA is used as a carbon source, controlling DA oxidation could have beneficial implications by improving electron transfer within the carbon structures [31, 32]. In these cases, borax can act as an inexpensive antioxidant for controlling DA functionalization or controlled polymerization. Addition of GSH is a viable option for both long-term and short-term sample preparation and storage for both benchtop and in vitro experiments. For biological applications, nitrogenation (or oxygen removal) is untenable, as it is conducive to cell hypoxia and atrophy. Similarly, the toxicity of borax limits its use for cell-based studies. Therefore, the use of GSH as antioxidant should be considered for biological assays.

2.3 In vitro cytocompatibility of DA

Preventing DA oxidation is critical for a number of biomedical applications due to potential oxidative stress–induced cytotoxicity [33]. Thus, we investigated the impact of DA when protected with an antioxidant (GSH) on the viability and metabolic activity of mammalian cells. To that end, 3T3 fibroblasts were cultured in complete cell culture media alone (0D) or in combination with either 1 mM DA (1D), 1 mM DA + 20 mM GSH (D20G), or 1 mM DA + 1 mM AA (D1A) for 24 h at 37 °C. Prior to cell culture, these solutions were

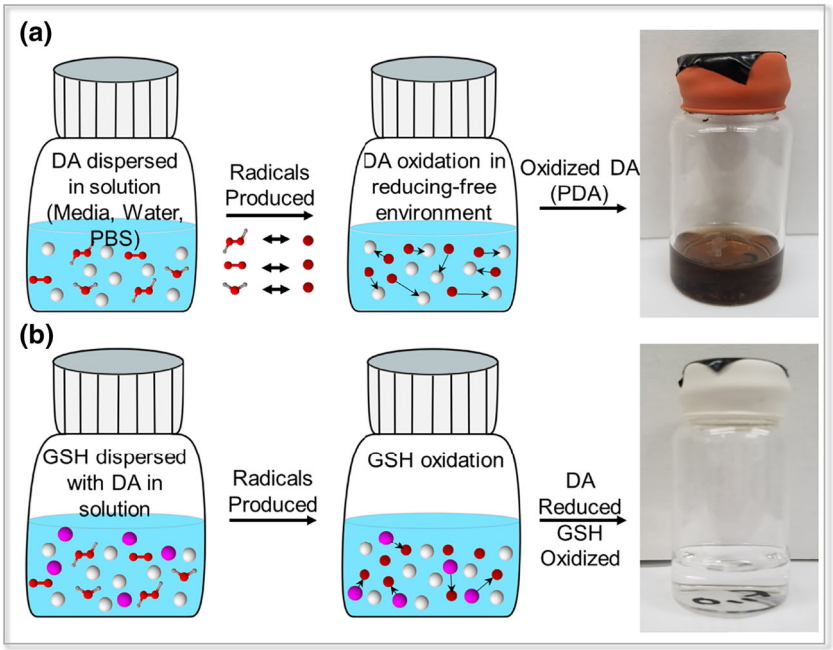

Fig. 4 Glutathione (GSH) prevents DA oxidation. **a** DA oxidation in antioxidant-free aqueous solutions leads to neuromelanin pigment formation and darkening. **b** GSH prevents DA oxidation resulting in colorless solutions, confirming the stability of DA

incubated for 1, 3, 5, 7, and 14 days at 37 °C. As expected, antioxidant-free DA showed a high cytotoxicity with cell viabilities of only 46.7% ± 2.11%, 15.8% ± 3.22%, and 11.1% ± 2.04% after 1, 3, and 5 days, respectively. Furthermore, all cells died after 7 days (Fig. 5a, b), as compared with the control (fibroblasts cultured in a DA-free media). Preventing DA oxidation using 20 mM GSH significantly increased cell viability to 87.3% ± 3.98%, 83.6% ± 6.97%, 78.3% ± 7.63%,

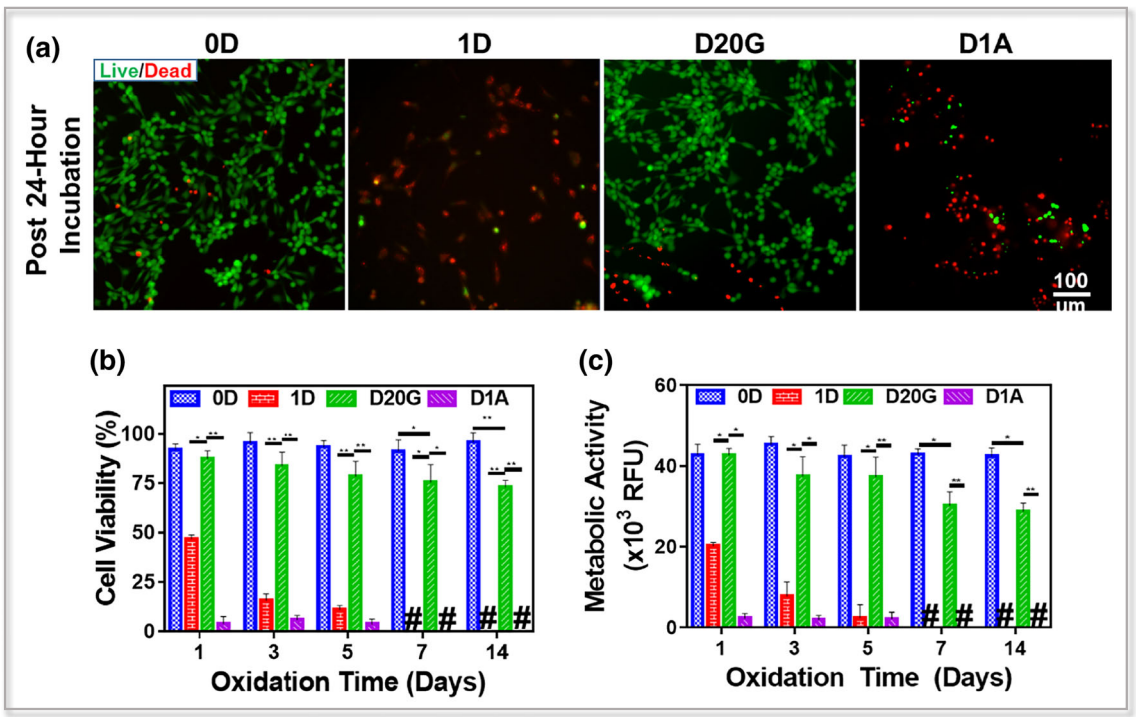

Fig. 5 GSH-protected DA retains high cell viability and metabolic activity. **a** Confocal images of 3T3 fibroblasts showing fractions of live (green) and dead (red) cells when cultured for 24 h in a DA-free cell culture media (0D) or in cell culture media supplemented with 1 mM DA (1D), 1 mM DA + 20 mM GSH (D20G), or 1 mM DA + 1 mM AA (D1A). Pretreated DA solutions were allowed to sit for 1, 3, 5, 7, and 14 days prior to be mixed with the cell culture media and be exposed to cells. **b** Quantification of 3T3 cell viability and (**c**) metabolic activity following 24 h incubation with the following cell culture media: 0D, 1D, D20G, and D1A. The number sign means no cells. Values represent mean and SD ($n = 3$). $p < 0.05$

75.3% ± 8.85%, and 72.9% ± 3.32% after 1, 3, 5, 7, and 14 days of culture, respectively. Nevertheless, low levels of cytotoxicity were observed. This was attributed to antioxidant exhaustion over time leading to partial DA oxidation. This was further evidenced by the negligible cytotoxicity observed when 3T3 cells were cultured in DA-free media supplemented with 20 mM GSH (20G) (Figure S6). Surprisingly, using 1 mM of AA (gold standard antioxidant) to prevent DA oxidation did not improve cell viability but rather increased cell death. Fibroblast viability was 4.03% ± 3.7%, 5.89% ± 2.31%, and 3.76% ± 2.64% after 1, 3, and 5 days, respectively. Furthermore, all cells died after 7 days. This is likely due to AA cytotoxicity, which is in accordance with the observed poor 3T3 cell survival when cultured in DA-free media supplemented with 1 mM AA (1A) (Figure S6). This observation is also in agreement with previously published reports showing the high cell toxicity and necrosis-mediated cell death induced by AA concentrations between 1 and 4 mM [34].

To confirm these results, the metabolic activity of 3T3 fibroblasts was assessed over time as shown in Fig. 5c. Cells were cultured in cell culture media supplemented with DA and various antioxidants (0D, 1D, D20G, or D1A). Fibroblasts treated with 1D dramatically reduced their metabolic activity by 52.7%, 82.7%, 94.1%, and 100% after 1, 3, 5, and 7 and 14 days, respectively. However, cells treated with D20G significantly improved cell metabolism, with up to 70% of metabolic activity preserved even after 14 days. In agreement with the cell viability data, 1 mM AA even further reduced cell metabolic activity when compared with 1D, with an 18-fold and a 22-fold decrease after 1 day and 3 days, respectively. The cytotoxicity of AA limited its use in biological systems at concentrations that are effective to prevent DA oxidation. Alternatively, GSH appeared to be a powerful and cell-friendly antioxidant. This is probably due to the suppression or reduction of DA-mediated oxidative stress by scavenging free radicals such as reactive oxygen species (ROS). Oxidized DA is known to trigger cytotoxicity and necrosis via deposition of DA quinone and other catechol derivatives on proteins, altering their function [33].

Several studies have shown that DA is also a regulator of T cell physiology and, in turn, immune responses [33, 35]. However, oxidation of DA resulted in the generation of ROS, which are believed to alter T cell function and proliferation. For this reason, low concentrations of ROS are a prerequisite for maintaining T cell survival [35]. To demonstrate the potential of GSH to prevent dopaminergic-triggered apoptosis, murine spleen–derived primary T cells were cultured (200,000 cells/mL, 1 mL per well of a 24-well plate) in complete cell culture media alone (0D) or in combination with either 1 mM DA (1D), 1 mM DA with 20 mM GSH (D20G), or 1 mM DA supplemented with 1 mM AA (D1A). Samples including 1D, D20G, and D1A were incubated for 1, 3, and 5 days at 37 °C prior to being exposed to T cells. After 24 h of incubation, T cell viability was determined by flow cytometry using a far-red fixable dead cell staining. While T cells cultured in 0D maintained a high viability for 24 h, T cells treated with 1D exhibited decreased cell viability, showing nearly complete cell death after 5 days (Fig. 6a, b). As expected, T cells cultured in the presence of D20G displayed increased cell viability (> 80%), up to 821-fold when compared with DA after 5 days of incubation. Conversely, T cells treated with D1A showed a dramatic decrease in cell viability with nearly complete cell death after 5 d of incubation. These results are in agreement with the data on cytotoxicity and metabolic activity of 3T3 cells, and further confirmed the capacity of GSH to prevent DA oxidation and ultimately oxidative stress–induced cell death.

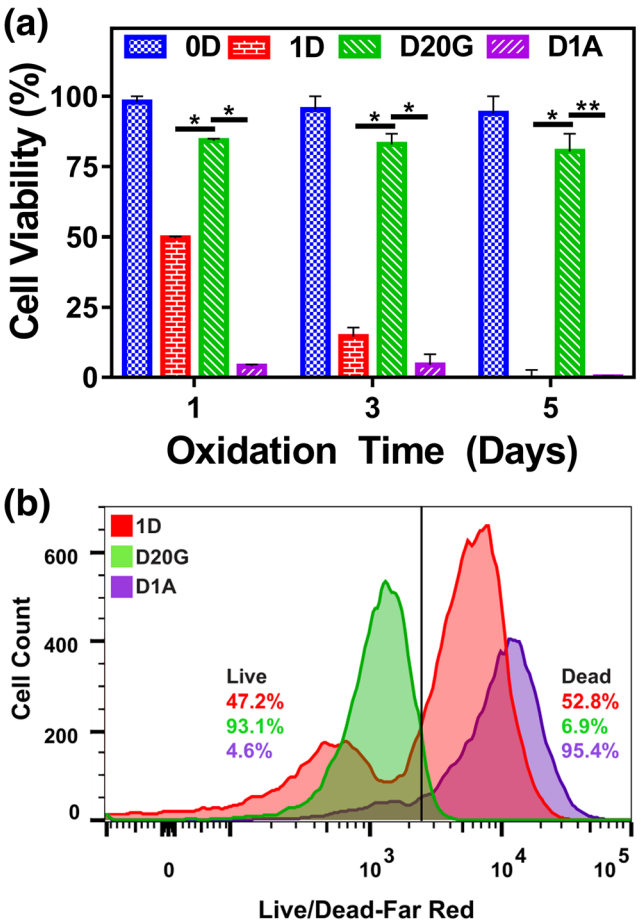

Fig. 6 GSH-protected DA preserves high T cell viability. **a** First, DA-containing solutions were subjected to oxidation for 1, 3, and 5 days. Next, T cells were incubated for 24 h with the pretreated DA-containing conditions: DA-free RPMI media (0D, control) and in RPMI media supplemented with 1 mM DA (1D), 1 mM DA + 20 mM GSH (D20G), and 1 mM DA + 1 mM AA (D1A). **b** Representative histogram of $CD3^+$ T cell viability after 24 h of incubation in RPMI media that was pretreated for 24 h with 1D, D20G, and D1A using far-red fixable dead staining. The histograms show one representative experiment of triplicate treatment. The number sign # means no cells. Values represent mean and SD ($n = 3$). $p < 0.05$

3 Conclusion

Overall, we demonstrate three simple approaches to stabilize DA and prevent or reduce its rapid oxidation. These strategies are useful to extend DA lifetime and prevent oxidative stress caused by its degradation. Our set of data demonstrates that GSH, especially at high concentrations (up to 20 mM), substantially prevents oxidation of DA (up to 99%) without any significant cytotoxicity. Unlike GSH, borax can provide a potential substitute when an antioxidant is utilized in amine-sensitive environments. Specifically, borax exhibits antioxidant properties in radical-rich environments due to its affinity for hydroxyl groups and its ability to form diester bridges between cis-hydroxyl-containing molecules [36]. Comparatively, GSH involves the sulfhydryl group of the cysteine interacting with radicals [37]. Finally, nitrogenation provides a supplementary preventive option, reinforcing DA protection against oxidation for up to 2 months. The strategies to prevent DA oxidation presented here can provide opportunities to further understand the activity of DA in its intact reduced state. The ability to prevent oxidation for extended periods of time (> 2 weeks) while retaining cytocompatibility has the potential to improve a number of biological studies, including interactions of DA in the nervous system [35]. Finally, preventing overoxidation of DA or its derivative, PDA, allows these molecules to retain sufficient functional groups and ultimately be used in tissue adhesive coatings and biomaterials

4 Materials and methods

4.1 Materials

Dopamine HCl, polydopamine, L-glutathione (98% purity; $C_{10}H_{17}N_3O_6S$), L-ascorbic acid ($C_6H_8O_6$), acetonitrile, tetraflouroacetic acid (TFA), and trypsin-edta and DMSO-D_6 were obtained from Millipore-Sigma (Burlington, MA, USA). Sodium tetraborate decahydrate (borax 99.5% purity, $Na_2(B_4O_5(OH)_4)\cdot 8H_2O$) was obtained from Thermo Fisher Scientific (Waltham, MA, USA). All chemicals were used without further purification. Dulbecco's Modification of Eagle's Medium (DMEM) and Roswell Park Memorial Institute (RPMI) medium were obtained from Corning Life Sciences (Corning, NY, USA) and supplemented with 10% *v*/*v* fetal bovine serum (Fisher Scientific), 100 μg/mL penicillin (Fisher Scientific), and 100 μg/mL streptomycin (Fisher Scientific) to form complete DMEM and RPMI cell culture media (50 μM β-mercaptoethanol (Fisher Scientific)). Fluorescent dyes, calcein AM and propidium iodide, were both purchased from GeneCopoeia (Rockville, MD, USA). Dopamine ELISA kit (KA1887) was obtained from Novus Biologicals (Littleton, CO, USA). T cell viability was analyzed using flow cytometry (BD FACSCalibur DXP Upgraded, Cytek Biosciences) using ViaQuant™ fixable red dead cell staining (GeneCopoeia; Rockville, MD, USA) and anti-mouse CD3 antibody (17A2, FITC). Fibroblast 3T3 cells were labeled using a ViaQuant™ Viability/Cytotoxicity Kit for Animal Cells (GeneCopoeia) using the manufacturer's protocol by fluorescent microscopy (Zeiss Axio Observer Z1 inverted microscope). Finally, 3T3 cell metabolic activity was observed and were imaged using after 1-day treatment (total post-seeding time of 2 days) using Cell-QuantTM AlamarBlue Cell Viability Reagent following manufacturer's protocol.

4.2 ^{1}H NMR characterization of DA

Solutions of DA, PDA, and GSH in 1 mL DMSO-D_6 were each prepared in a Bruker Biospin disposable NMR tube following protocol developed elsewhere [10]. The respective ^{1}H NMR spectra were collected on a 400-MHz Varian NMR spectrometer and evaluated by integrating peaks between δ5.6 and 5.8 ppm, corresponding to CH (Figure S1a) of the benzene ring, and peaks at δ1.8 and δ2.0 ppm, corresponding to CH2 (Figure S1b, c) in DA. Similarly, shifts between δ6.5 and 7.5 ppm were assigned to the H surrounding both the benzene and pyrrole functional groups [38]. Finally, a shift at δ1.6 ppm corresponded to the hydrogen-amine bonds in the alkene chain in DA and the hydrogen-nitrogen bonds in the pyrrole group.

4.3 High-performance liquid chromatography of DA

To make a DA stock solution, 20 mg of DA was dissolved in 1 mL of PBS and the pH was adjusted to 8.30 as previously reported [25]. This stock solution was then diluted to make a 1 mM DA in PBS solution. In addition, both GSH (20 mM) and control PDA (1 mM) were each dissolved in 1 mL of PBS. The HPLC analyses were performed on an Agilent 1100 Series HPLC with quaternary pump, auto sampler, and UV detector equipped with a Discovery BIO Wide Pore C18 HPLC column (3-μm particle size; L, 5 cm; ID, 0.5 mm; Supelco Analytical a Millipore-Sigma Division, Burlington, MA, USA). The mobile phase was made up of MilliQ water with 0.1% TFA and acetonitrile in 0.1% TFA in an optimized ratio of 30:70, respectively. The various analytes were detected using UV-vis (280 nm) at a flow rate of 0.3 mL/min. Elution times for DA and PDA were detected at 5 min and 14.4 min, respectively, following UV absorbance [25]. Amount of DA by percentage was obtained by relating the relative intensities of each peak to a known concentration (i.e., 1 mM DA).

4.4 Raman and Fourier-transform infrared spectroscopy of DA oxidation

Raman spectroscopy was performed using a Thermo Scientific DXR2xi Raman imaging microscope with an

excitation wavelength of 785 nm, a resolution of 5 cm^{-1}, and a beam diameter of 10 mm. Spectra were evaluated at 1485 cm^{-1} and 1525 cm^{-1} for the presence or disappearance of quinone and pyrrole groups, respectively. Fourier-transform infrared (FTIR) spectroscopy was obtained using a Bruker Vertex 70 spectrometer. Spectra were evaluated at 2150 cm^{-1} and 3150–3600 cm^{-1} for the presence or disappearance of the C–N–C and pyrrole groups, respectively.

4.5 DA oxidation study

Oxidation studies were conducted in 20-mL scintillation vials equipped with rubber precision seal septum. Briefly, for the controls, 1 mM DA ± antioxidant was dissolved either in 5 mL of water or PBS; after which, the vials were properly sealed. Samples were then monitored over 56 days and samples were collected for UV-vis analysis. Absorbance measurements of samples were recorded at (day 0) and after 1, 3, 7, 14, 28, and 56 days and the percent of DA oxidation was calculated from UV absorbance at 530 nm. For nitrogenated samples, 5 mL of water or PBS in scintillation vials was sealed with rubber seals and subsequently purged with nitrogen for 30 min. A total of 1 mM DA with or without antioxidants were then added into the vials using a syringe followed by 30 min of purging with nitrogen to ensure an oxygen-free sample prior to studies. Samples were then monitored over 56 days and measured as described above. A control sample containing 1 mM PDA in PBS was taken as 100% oxidized. All absorbance values were then scaled to control 1 mM PDA absorbance to represent 100% DA oxidation and the set of data was used to determine corresponding oxidation kinetics.

4.6 DA enzyme-linked immunosorbent assay

After 1, 3, and 5 days of DA oxidation at 37 °C and humidified at 5% CO_2, 1 μL of a solution of 1 mL PBS with 1 mM DA, 1 mM DA supplemented with 20 mM GSH, or 1 mM DA supplemented with 1 mM AA was collected, diluted 1000×, and then the concentration of DA was analyzed using a DA ELISA kit, according to the manufacture's guidelines.

4.7 DA stability in cell culture media

An assessment of DA stability was performed to evaluate the potential oxidation of DA in media prior to any cytotoxicity studies. Briefly, 1 mM DA solution was added to DMEM containing different concentrations of GSH (1, 5, 10, and 20 mM) and AA (1 and 20 mM). Next, DA was monitored both visually and by UV-vis spectroscopy at 530 nm over a 7-day period. Plain media was used as control. Samples were incubated at 37 °C with 5% CO_2.

4.8 In vitro cytotoxicity studies

Mouse fibroblasts (NIH/3T3, CRL-1658, ATCC, Rockville, MD, USA) were cultured in complete DMEM at 37 °C in a humidified 5% CO_2/95% air containing atmosphere. Splenocytes were isolated from C57BL/6 mice and cultured in complete RPMI. For viability studies, cells were seeded in a 24-well plate (200,000 cells/mL of complete media) for 24 h prior to incubation with the different conditions. All DA-containing conditions were subjected to oxidation for 1, 3, and 5 days before utilization. Conditions were as follows: no DA control (0D), 1 mM DA (1D), 1 mM DA with 10 mM GSH (D10G), 1 mM DA with 20 mM GSH (D20G), 1 mM DA with 1 mM AA (D1A), and 1 mM DA with 20 mM AA (D20A). The conditions were prepared in appropriate media (DMEM for fibroblasts, RPMI for T cells). Live/dead imaging and viability was determined using a ViaQuant Viability/Cytotoxicity Kit for Animal Cells (GeneCopoeia no. A017) according to the manufacturer's protocol. Briefly, post-incubation for 24 h cells were washed with PBS and stained with propidium iodide and calcein AM followed by more PBS washing. The stained cells were immediately imaged on a Zeiss Axio Fluorescent Microscope. Images were then processed via ImageJ image processing software to filter and count stained cells. The percentage of viable cells was determined as the ratio of viable cells to total number of cells. T cell viability was analyzed using flow cytometry (BD FACS Calibur DXP Upgraded, Cytek Biosciences) using ViaQuant™ fixable red dead cell staining (GeneCopoeia; Rockville, MD, USA; 640 nm) and anti-mouse CD3 antibody (17A2, FITC; 488 nm). Cell metabolic activity (MA) was conducted using a standard AlamarBlue assay (Thermo Fisher Scientific). Briefly, 100 μL of media was removed from a 24-well plate containing cells with media and replaced with 100 uL of AlamarBlue. MA was measured via fluorescence at 530–560 nm using an HTS-XT microplate reader.

4.9 Statistical analysis

Data analysis was carried out using a 1-way ANOVA test with GraphPad Prism 6.0 software. Error bars represent mean ± standard deviation (SD) of measurements ($*p < 0.05$, $**p < 0.01$).

Funding information S.A.B. received support from the Northeastern University Seed Grant/Proof of Concept Tier 1 Research Grant, Burroughs Wellcome Fund (BWF) award, Thomas Jefferson/Face foundations award, DFCI/NU Joint Program Grant, and NSF CAREER award (1847843). N.A. acknowledges the support from the American Heart Association (AHA, 16SDG31280010) and the National Institutes of Health (NIH) (R01EB023052; R01HL140618), Northeastern University, and the startup funds provided by the Department of Chemical Engineering, College of Engineering at Northeastern University.

References

1. D.J. F, K.M. Gray, Pharmacology and therapeutic use of low-dose dopamine. Pharmacotherapy: The Journal of Human Pharmacology and Drug Therapy **6**, 304–310 (1986)
2. B.M. Varsha, N.M. C, Dopamine and dobutamine in pediatric therapy. Pharmacotherapy **9**, 303–314 (1989)
3. L.Y.W. Francis, Clinical pharmacology of dopamine agonists. Pharmacotherapy **20**, 17S–25S (2000)
4. R. Myung-Hyun, L.Y. Min, P. Jung-Ki, C.J. Wook, Mussel-inspired polydopamine-treated polyethylene separators for high-power Li-ion batteries. Adv. Mater. **23**, 3066–3070 (2011)
5. Y. Liu, K. Ai, L. Lu, Polydopamine and its derivative materials: synthesis and promising applications in energy, environmental, and biomedical fields. Chem. Rev. **114**, 5057–5115 (2014)
6. D.G. Graham, S.M. Tiffany, F.S. Vogel, The toxicity of melanin precursors. J. Investig. Dermatol. **70**, 113–116 (1978)
7. B. Uttara, A.V. Singh, P. Zamboni, R.T. Mahajan, Oxidative stress and neurodegenerative diseases: a review of upstream and downstream antioxidant therapeutic options. Curr. Neuropharmacol. **7**, 65–74 (2009)
8. M. Lalkovičová, V. Danielisová, Neuroprotection and antioxidants. Neural Regen. Res. **11**, 865–874 (2016)
9. Y. Cong, T. Xia, M. Zou, Z. Li, B. Peng, D. Guo, Z. Deng, Mussel-inspired polydopamine coating as a versatile platform for synthesizing polystyrene/Ag nanocomposite particles with enhanced antibacterial activities. J. Mater. Chem. B **2**, 3450–3461 (2014)
10. J. Liebscher, R. Mrówczyński, H.A. Scheidt, C. Filip, N.D. Hădade, R. Turcu, A. Bende, S. Beck, Structure of polydopamine: a never-ending story? Langmuir **29**, 10539–10548 (2013)
11. Z. Gao, L. Duan, Y. Yang, W. Hu, G. Gao, Mussel-inspired tough hydrogels with self-repairing and tissue adhesion. Appl. Surf. Sci. **427**, 74–82 (2018)
12. L. Han, X. Lu, K. Liu, K. Wang, L. Fang, L.-T. Weng, H. Zhang, Y. Tang, F. Ren, C. Zhao, G. Sun, R. Liang, Z. Li, Mussel-inspired adhesive and tough hydrogel based on nanoclay confined dopamine polymerization. ACS Nano **11**, 2561–2574 (2017)
13. Y. Yang, P. Qi, Y. Ding, M.F. Maitz, Z. Yang, Q. Tu, K. Xiong, Y. Leng, N. Huang, A biocompatible and functional adhesive amine-rich coating based on dopamine polymerization. J. Mater. Chem. B **3**, 72–81 (2015)
14. R.H. Siddique, Y.J. Donie, G. Gomard, S. Yalamanchili, T. Merdzhanova, U. Lemmer, H. Hölscher, Bioinspired phase-separated disordered nanostructures for thin photovoltaic absorbers. Sci. Adv. **3**, e1700232 (2017)
15. E. Mazario, J. Sanchez-Marcos, N. Menendez, P. Herrasti, M. Garcia-Hernandez, A. Munoz-Bonilla, One-pot electrochemical synthesis of polydopamine coated magnetite nanoparticles. RSC Adv. **4**, 48353–48361 (2014)
16. M.-V. Clement, L.H. Long, J. Ramalingam, B. Halliwell, The cytotoxicity of dopamine may be an artefact of cell culture. J. Neurochem. **81**, 414–421 (2002)
17. D. Offen, I. Ziv, S. Gorodin, A. Barzilai, Z. Malik, E. Melamed, Dopamine-induced programmed cell death in mouse thymocytes. Biochim. Biophys. Acta (BBA) Mol. Cell Res. **1268**, 171–177 (1995)
18. J. Segura-Aguilar, I. Paris, in *Handbook of Neurotoxicity*, ed. by R. M. Kostrzewa. (Springer New York, New York, NY, 2014), pp. 865–883
19. B. Halliwell, Oxidative stress in cell culture: an under-appreciated problem? FEBS Lett. **540**, 3–6 (2003)
20. J.K. Andersen, Oxidative stress in neurodegeneration: cause or consequence? Nat. Rev. Neurosci. **10**, S18 (2004)
21. L. Shi, S. Santhanakrishnan, Y.S. Cheah, M. Li, C.L.L. Chai, K.G. Neoh, One-pot UV-triggered o-nitrobenzyl dopamine polymerization and coating for surface antibacterial application. ACS Appl. Mater. Interfaces **8**, 33131–33138 (2016)
22. D. Offen, I. Ziv, H. Sternin, E. Melamed, A. Hochman, Prevention of dopamine-induced cell death by thiol antioxidants: possible implications for treatment of Parkinson's disease. Exp. Neurol. **141**, 32–39 (1996)
23. Y.H. Ding, M. Floren, W. Tan, Mussel-inspired polydopamine for bio-surface functionalization. Biosurface Biotribol. **2**, 121–136 (2016)
24. M. Bisaglia, S. Mammi, L. Bubacco, Kinetic and structural analysis of the early oxidation products of dopamine: analysis of the interactions with α-synuclein. J. Biol. Chem. **282**, 15597–15605 (2007)
25. S. Hong, Y.S. Na, S. Choi, I.T. Song, W.Y. Kim, H. Lee, Non-covalent self-assembly and covalent polymerization co-contribute to polydopamine formation. Adv. Funct. Mater. **22**, 4711–4717 (2012)
26. H. Sies, Oxidative stress: a concept in redox biology and medicine. Redox Biol. **4**, 180–183 (2015)
27. H. Liu, T.A. Bruton, F.M. Doyle, D.L. Sedlak, In situ chemical oxidation of contaminated groundwater by persulfate: decomposition by Fe(III)- and Mn(IV) containing oxides and aquifer materials. Environ. Sci. Technol. **48**, 10330–10336 (2014)
28. P. Munoz, S. Huenchuguala, I. Paris, J. Segura-Aguilar, Dopamine oxidation and autophagy. Park. Dis. **2012**, 13 (2012)
29. W.D. Bush, J. Garguilo, F.A. Zucca, A. Albertini, L. Zecca, G.S. Edwards, R.J. Nemanich, J.D. Simon, The surface oxidation potential of human neuromelanin reveals a spherical architecture with a pheomelanin core and a eumelanin surface. Proc. Natl. Acad. Sci. **103**, 14785–14789 (2006)
30. M.E. Rice, Ascorbate regulation and its neuroprotective role in the brain. Trends Neurosci. **23**, 209–216 (2000)
31. V. Veeramani, R. Madhu, S.-M. Chen, M. Sivakumar, Flower-like nickel-cobalt oxide decorated dopamine-derived carbon nanocomposite for high performance supercapacitor applications. ACS Sustain. Chem. Eng. **4**, 5013–5020 (2016)
32. C. Lei, F. Han, D. Li, W.-C. Li, Q. Sun, X.-Q. Zhang, A.-H. Lu, Dopamine as the coating agent and carbon precursor for the fabrication of N-doped carbon coated Fe3O4 composites as superior lithium ion anodes. Nanoscale **5**, 1168–1175 (2013)
33. I. Miyazaki, M. Asanuma, *Dopaminergic neuron-specific oxidative stress caused by dopamine Itself*, vol 62 (2008), pp. 141–150
34. S.J. Padayatty, A. Katz, Y. Wang, P. Eck, O. Kwon, J.-H. Lee, S. Chen, C. Corpe, A. Dutta, S.K. Dutta, M. Levine, Vitamin C as an antioxidant: evaluation of its role in disease prevention. J. Am. Coll. Nutr. **22**, 18–35 (2003)
35. P. Kesarwani, A.K. Murali, A.A. Al-Khami, S. Mehrotra, Redox regulation of T-cell function: from molecular mechanisms to significance in human health and disease. Antioxid. Redox Signal. **18**, 1497–1534 (2013)
36. I. Yerbolat Maratovich, K. Nurgul Narimanovna, I. Irina Vladimirovna, I. Marat Kapenovich, Protective action of sodium tetraborate on chrom-induced hepato- and genotoxicity in rats. Biomed. Pharmacol. J. **10**, 1239–1247 (2017)
37. H.J. Forman, H. Zhang, A. Rinna, Glutathione: overview of its protective roles, measurement, and biosynthesis. Mol. Asp. Med. **30**, 1–12 (2009)
38. D.R. Dreyer, D.J. Miller, B.D. Freeman, D.R. Paul, C.W. Bielawski, Elucidating the structure of poly(dopamine). Langmuir **28**, 6428–6435 (2012)